GA–A23892

RESISTIVE WALL MODE CONTROL ON THE DIII–D DEVICE

by
M. OKABAYASHI, J. BIALECK, M.S. CHANCE, M.S. CHU,
E.D. FREDRICKSON, A.M. GAROFALO, R. HATCHER, T.H. JENSEN,
L.C. JOHNSON, R.J. LAHAYE, M.A. MAKOWSKI, G.A. NAVRATIL,
E.A. LAZARUS, J.T. SCOVILLE, E.J. STRAIT, A.D. TURNBULL,
M.L. WALKER, and the DIII–D TEAM

DECEMBER 2001

DISCLAIMER

GA–A23892

RESISTIVE WALL MODE CONTROL ON THE DIII–D DEVICE

by
M. OKABAYASHI,* J. BIALECK,† M.S. CHANCE,* M.S. CHU,
E.D. FREDRICKSON,* A.M. GAROFALO,† R. HATCHER,* T.H. JENSEN,
L.C. JOHNSON,* R.J. LAHAYE, M.A. MAKOWSKI,‡ G.A. NAVRATIL,†
E.A. LAZARUS,¶ J.T. SCOVILLE, E.J. STRAIT, A.D. TURNBULL,
M.L. WALKER, and the DIII–D TEAM

This is a preprint of an invited paper to be presented at the Joint Conference of the 12th International Toki Conference on Plasma Physics and Controlled Nuclear Fusion and the 3rd General Scientific Assembly of Asia Plasma Fusion Association, December 11–14, 2001, Toki, Japan and to be published in *Journal of Plasma and Fusion Research.*

*Princeton Plasma Physics Laboratory, Princeton, New Jersey.
†Columbia University, New York, New York.
‡Lawrence Livermore National Laboratory, Livermore, California.
¶Oak Ridge National Laboratory, Oak Ridge, Tennessee..

Work supported by
the U.S. Department of Energy under
Grant No. DE-FG02-89ER53297 and Contract Nos.
DE-AC03-99ER54463, DE-AC02-76CH03073, W-7405-ENG-48,
and DE-AC05-00OR22725

GENERAL ATOMICS PROJECT 30033
DECEMBER 2001

Resistive Wall Mode Control on the DIII–D Device

OKABAYASHI Michio,[1] BIALEK James,[2] CHANCE Morrell,[1] CHU Ming,[3] FREDRICKSON Eric,[1] GAROFALO Andrea,[2] HATCHER Ronald,[1] JENSEN Torkil,[3] JOHNSON Larry,[1] LA HAYE Robert,[2] LAZARUS Edward,[4] MANICKAM Janardhan,[1] NAVRATIL Gerald,[2] SCOVILLE John Tim,[3] STRAIT Edward,[3] TURNBULL Alan,[3] WALKER Michael,[3] and DIII-D Team

1) Princeton Plasma Physics Laboratory, Princeton, New Jersey.

2) Columbia University, New York, New York.

3) General Atomics, P.O. Box 85608, San Diego, California 92186-5608.

4) Oak Ridge National Laboratory, Oak Ridge, Tennessee.

e-mail: mokabaya@pobox.pppl.gov

Abstract

External kink modes have been identified as one of the major obstacles to achieving high pressure plasmas in toroidal devices. From the beginning of fusion research, it has been well known that a conducting shell can improve the stability if the shell is ideal. A shell with finite resistivity can still stabilize the fast growing ideal magnetohydrodynamic (MHD) mode, however, the external kink mode is converted into the resistive wall mode (RWM) branch, which grows with the shell skin time constant.

On the DIII-D device, two schemes have been explored to stabilize the slowly-growing resistive wall mode: one using magnetic feedback and the other utilizing rapid plasma rotation. Recent RWM experiments have revealed that these two schemes are strongly coupled in a synergetic manner and that the stabilization operation functions as a unified scheme. It was found that the magnetic feedback operation can track the residual error field which excites the stable resistive wall mode near the marginally stable condition (Error Field Amplification). The magnetic field applied through the feedback process can reduce the mode amplitude, compensate the error field, and simultaneously maintain the plasma rotation. As a consequence of the higher plasma rotation, a stable path opens up to the ideal-wall limit. Discharges with beta up to twice the no-wall beta limit have been achieved. Experimental observations and stability calculations indicate that these discharges are at the ideal wall kink limit.

Keywords: external kinks, resistive wall mode, ideal MHD, error field

1. Introduction

The external kink mode has been considered as one of most dangerous obstacles which may hinder us from achieving commercially-attractive fusion reactors. Numerous experiments have consistently indicated that external kink modes are a major cause of the currently achievable plasma pressure limit in toroidal devices.

The efficacy of the conducting shell has been demonstrated in early tokamaks, and RFPs. The presence of a conducting shell reduces the growth rate and the shell-stabilized plasmas transiently have achieved higher beta [1–3]. Since the wall with finite resistivity loses the flux-conserving stabilizing force in time, the external kink instability is branched into the resistive wall mode (RWM) [4]. Since

the RWM mode exhibits a sufficiently slow growth rate, various approaches are possible to suppress or control the mode amplitude. Over the last decades, the magnetic feedback stabilization has been considered as a possible and economical cure even in reactor oriented devices [5]. Recently a scheme with the plasma rotation through kinetic dissipation has been proposed as an alternative [6,7]. These approaches are shown schematically in Fig. 1. Recent experiments in DIII-D have shown the feasibility of both feedback stabilization [8] and rotational stabilization [9].

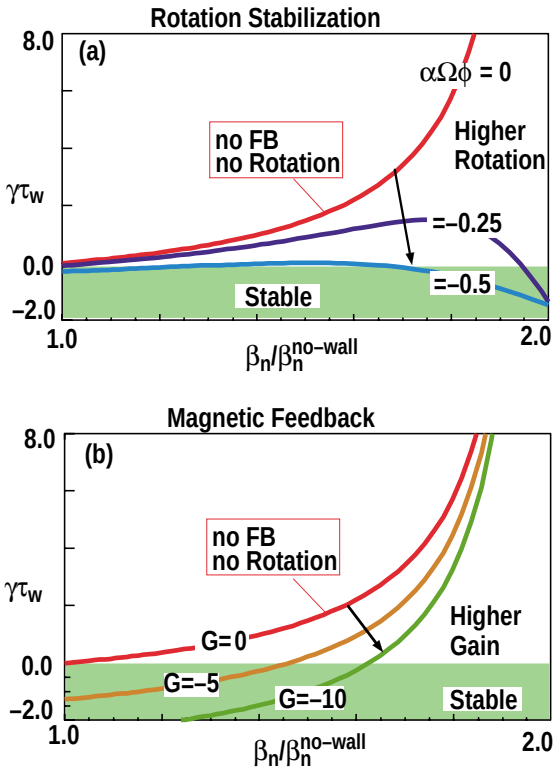

Fig. 1. Schematic diagrams of RWM stabilization. (a) Magnetic feedback stabilization with a control logic "smart shell". (b) Rotational stabilization without magnetic feedback. Ω_ϕ is the plasma angular rotation frequency and α represents the magnitude of dissipation relative to the plasma potential energy. $\beta_N/\beta_N^{\text{no wall}} = 1.0$ corresponds to the no-wall limit and $\beta_N/\beta_N^{\text{no wall}} = 2.0$ corresponds to the ideal-wall limit.

On the DIII-D device, it has been discovered that both magnetic feedback and rotation stabilization successfully function in a synergetic manner to reduce the RWM amplitude, maintain the plasma rotation, and establish a high $\beta_N = \beta/(B_T/aI_P)$ configuration (where the β is the ratio of plasma pressure to the toroidal magnetic pressure). A key factor is the discovery of excitation of stable RWMs by a residual error field [9,10] (Error Field Amplification), predicted by Boozer [11]. Near the marginal condition, the residual error field excites the stable RWM in a helically-resonant manner, causing a strong drag on the plasma rotation. Often this leads to rotational slowing and growth of the RWM [12]. Feedback which senses the mode tries to reduce the mode amplitude and consequently compensate the error field. As a consequence, the reduction of the error field prevents the dissipation of the toroidal angular momentum. When the plasma rotation is maintained above a critical value with sufficient angular momentum input sustained, the RWM is stabilized, which is consistent with a mechanism as discussed by Bondeson and Ward [6,7].

Once the proper error field compensation is found through the feedback operation, the error field correction applied without feedback can also produce high β_N configurations identical to the one with feedback applied. A key factor for the success of this scheme is the use of poloidal field sensors inside the vacuum vessel, which are primarily sensitive to the mode and insensitive to the applied normal field. Thus, the sensor observes more effectively the mode amplitude and phase in comparison to other sensors [8-10,13]. The other encouraging fact is that the improvement via maintaining the plasma rotation is obtainable in wide rage of plasma parameters such as quasi-steady state high β_N discharges [14]. The study with the MARS simulation code by [15,16] supports the observed sensor preference.

With these experimental results, a unified concept of RWM control has emerged from the magnetic and rotational stabilization schemes which were once considered as two "distinct" approaches. This synergetic nature for stabilizing the RWM both from magnetic and plasma rotation will open up a wide range of plasma parameters, which were once thought impractical if we were to rely only on one of them.

In this paper, we have summarize the recent progress of RWM control on the DIII-D device.

2. Resistive wall mode and error field amplification

2.1. Mode characteristics of RWM

The potentially dangerous external kink mode is converted into a RWM under the influence of the finite resistivity of the wall [4]. According to conventional theory, the RWM is considered as a mode which retains the ideal MHD kink character over many Alfvénic time scales. Because of the small growth rate ($\gamma \approx 1/\tau_w$) due to the resistive magnetic flux loss on the wall, the mode structure is expected to follow ideal MHD character except at resonance areas on q = integer surfaces [2,7]. The RWM has a global helical displacement extending from the core plasma to beyond the vacuum vessel. Any significant magnetic islands are not formed even though the global resonant helical distortion is significantly large (as much as 1%–2% of the equilibrium field on the plasma surface), and the mode often behaves like a quasi-stationary helical equilibrium. The existence of ideal kink nature over so long a time scale seems like an over simplified hypothesis. This seemingly puzzling character based on conventional ideal MHD predictions has necessitated series of experimental, theoretical, and numerical studies.

To address the issue of the mode structure under the influence of finite resistivity, theoretical and experimental efforts have been made during last a few years. A numerical study has been carried out with the GATO and DCON plasma stability code combined with the VACUUM code [17,18]. In these analyses, the resistive flux loss on the wall and its impact back to the plasma surface is treated in a self-consistent manner. The results indicate that the mode structure inside the plasma remains largely intact and that the eddy current pattern on the wall is not significantly modified [8,12,17,18].

On the DIII-D device, the mode structure has been studied with both a high resolution ECE spectrometer and two toroidally-separated soft x-ray arrays. The results indicate that the RWM evolves in time without creating any noticeable magnetic islands even when the mode amplitude observed outside the vessel reaches to the order of 5–10 gauss [8,10,13]. The slow time evolution of the observed mode inside the plasma coincides well with the flux time history observed outside the vacuum vessel. In addition, the radial flux measured at above/below mid-plane compared with the flux evolution at the midplane indicates that the mode behaves as one large rigid displacement with a helicity conserved.

Because of the slowly-growing nature, non-ideal effects may play a significant role as a cumulative effect for stabilizing the mode, while the instantaneous ideal MHD character still remains intact. Bondeson and Ward [6,7] proposed that the RWM can be stabilized by the dissipation due to plasma rotation if the plasma rotation is above a critical value, typically, a few percent of Alfvénic velocity. Possible causes for the mode dissipation have been proposed by various groups and the experimental study of these predictions has just begun. On DIII-D, several experiments have revealed that rapid RWM growth is coincided with sharp decrease of plasma rotation [12,19,20]. The higher angular momentum injection with NBI was carried out by careful adjustment of the neutral beam injection velocity with the total input power maintained at a constant value [8–10]. The plasma rotation was increased while holding the total stored energy constant at a plasma pressure just above the no-wall beta limit. When the plasma rotation was increased by 20%, the RWM onset was delayed by 100–200 ms. However, the RWM eventually grew, reduced the plasma rotation, and led to the beta collapse, indicating that the higher rotation alone was not sufficient for complete stabilization. Nonetheless, this experimental result suggests that plasma rotation is a major factor in achieving RWM control.

2.2. Error field amplification (EFA)

Boozer [11] proposed that when a plasma approaches the marginal stability condition,

namely, the no-wall beta limit against the external kink, the amplitude of the plasma distortion to a residual external perturbation (such as error field) increases inversely proportional to a torque parameter, plasma toroidal rotation. This effect has been termed error field amplification (EFA). The amplitude is larger near the onset condition. The helical distortion is balanced by the intrinsic field. Thus, this distortion has a linear dependence on the extra field like "amplification". Experimentally it was demonstrated [9] that when β_N approaches the marginal condition, the applied pulsed error field can induce the n=1 helical response (Fig. 2). Special care was made for this observation in order to have sufficient plasma rotation velocity and the extra error field low enough to avoid a reduction in plasma rotation. With β_N above the no-wall beta limit, $\beta_N^{\text{no wall}}$, the distortion is larger compared with the response at $\beta_N \approx \beta_N^{\text{no wall}}$. After the pulsed field was turned off, the mode decayed at the rate of $1/\tau_w$, indicating that the

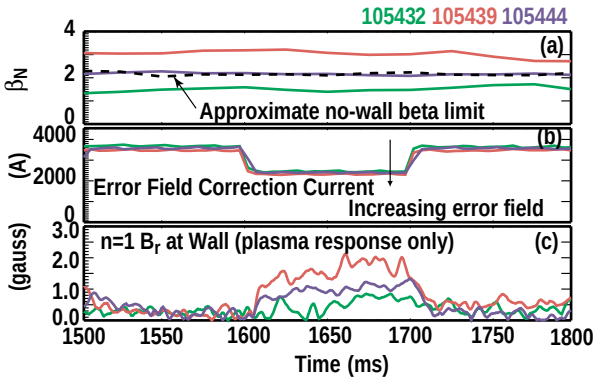

Fig. 2. Stable RWM excited with pulse field. The larger amplitude of EFA is induced with $\beta_N/\beta_N^{\text{no wall}} \geq 1.0$. Decay of the mode after the pulse field indicates that the plasma condition belongs to the stable regime. (a) β_N vs. time; (b) error field correction current vs. time. About 3 kA was needed to provide the optimal error field correction. Extra error field is applied by the sudden change of coil current. (c) The plasma response observed on the external δB_r saddle loop.

mode excited did belong to marginally stable regime. Figure 3(a,b) shows the EFA amplitude and phase for various β_N. summarized

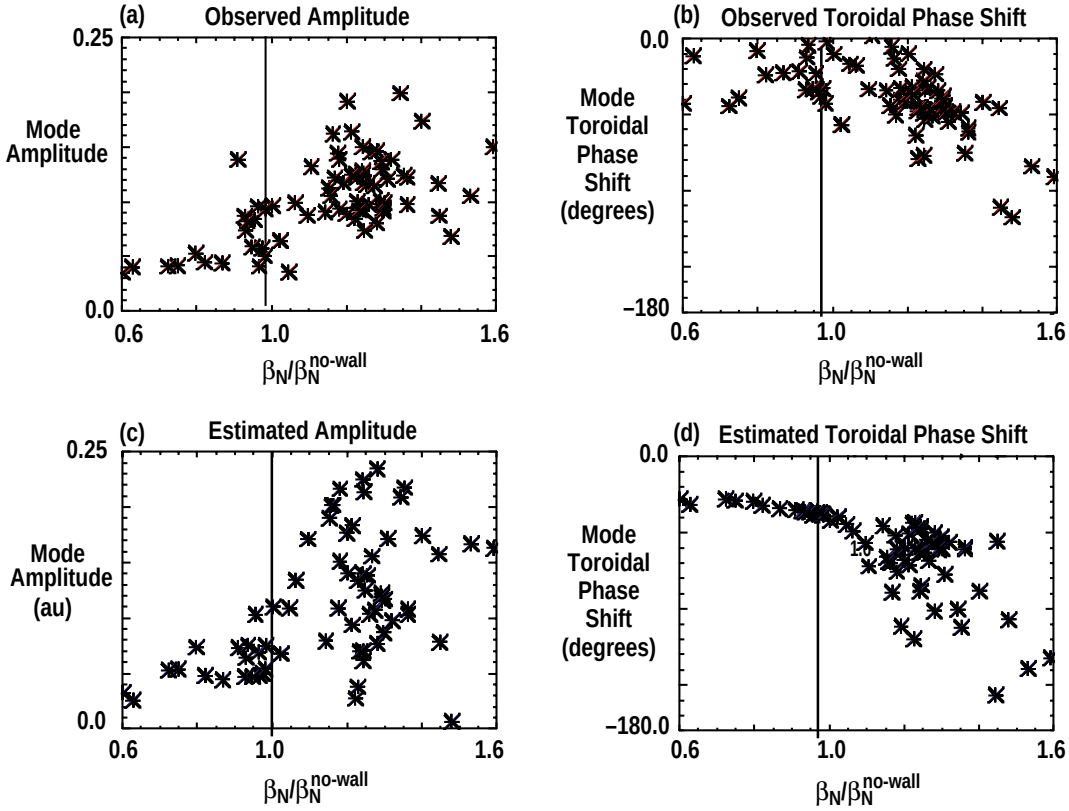

Fig. 3. EFA amplitude and toroidal phase (a) and (b): Experimental results. (c) and (d): Estimated values by Eq. (4) using the observed rotation velocity. The amplitude scale is in arbitrary unit.

from the pulsed field operation. Here, the EFA amplitude is defined as the helical n=1 flux due to the plasma perturbation, namely the total observed flux subtracted by the applied external field. The most important result is that there is a finite phase shift between the applied field and the excited mode. The phase shift is 20 degrees at $\beta_N \approx \beta_N^{\text{no wall}}$ and increases to 90–120 degrees at higher β_N. This toroidal phase shift of the plasma response should be taken into account for feedback operation. This had not been considered before this discovery.

When a larger extra error field is applied, the plasma rotation gradually decreases and once the velocity is below a critical value, the EFA becomes too strong, leading to rotational collapse. This indicates that the rotational stabilization requires a critical rotational velocity, which corresponds to ≈6 kHz for the present experimental condition. This value is not far from a critical velocity estimate given by [6,7]. Some experimental data is shown later.

3. Hardware for RWM control on DIII-D device

The power supply required for magnetic feedback is rather modest, since the RWM growth time is of the order of the resistive wall skin time τ_w, which is far slower than the Alfvénic time. The sensor geometry depends on the choice of control logic. The smart shell scheme is to control the total flux (including the flux supplied from the coil) by compensating the helical flux leakage of the wall and to build the virtual ideal shell on the wall [5]. The smart shell approach works best with δB_r saddle loop, which detects the flux decay over the shell surface. Another scheme is the mode control logic using the signal originating only from the plasma surface displacement and without coupling to the active coil current. The mode control logic works best with poloidal field sensors inside the vacuum vessel.

On DIII-D, various sensors have been installed inside and outside the vessel. Figure 4 shows a schematic diagram of sensor and active coil location. The details of sensor geometry are summarized in Table 1. Each saddle loop covers 60 toroidal degrees. The

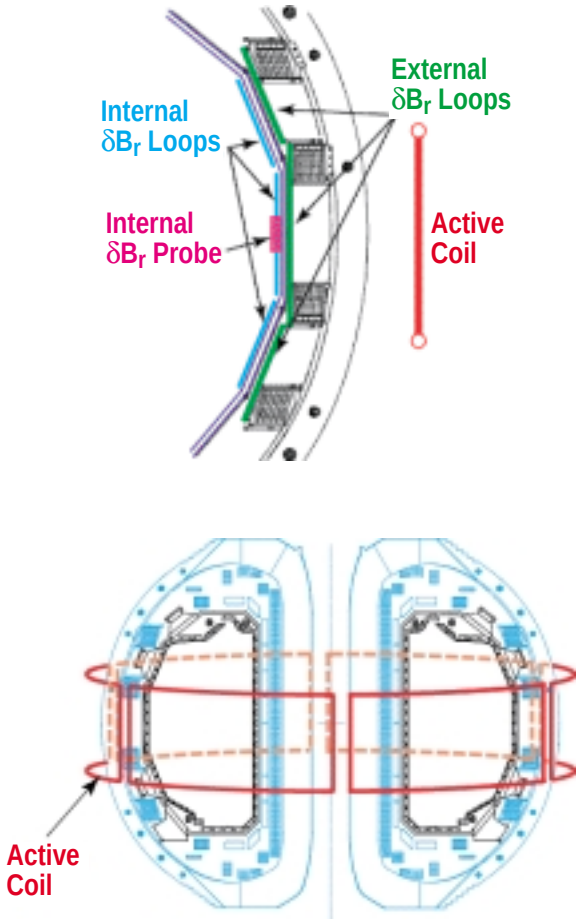

Fig. 4. Active coil geometry and sensor locations.

input signal to the feedback system is made by combining a pair of sensors located at toroidally opposed angles, to produce only n = odd components.

The active coils on DIII-D device have two roles: one is to compensate the error field and he other is to serve as the active feedback actuator. Present active coils are toroidally located in phase to the saddle flux loops. Coils located 180 degrees apart are also paired in anti-series so that only n = odd components are produced and are energized with current power supplies up to 5 kA with dc-100 Hz capability. A coil current of 1 kA produces 13 gauss radial field on the vacuum vessel. As shown later, about one half of the maximum current is used for error field correction. It should be noted that the applied active field does not have any helicity preference, since only one layer of coil exists in the poloidal direction.

Table I. Geometry of sensor and active coil

Sensors	Poloidal Coverage	Toroidal Combination	Toroidal Location (pair at degrees)	Type	Main Role
Outside δB_r saddle loop	Midplane	3 pairs	79, 139, 199	Bn	Control
	Above/below	6 pairs	64, 94, 124, 154, 184, 214	Bn	m determination
Inside δB_r saddle loop	Midplane	3 pairs	74, 133, 198	Bn	Control
	Above/below	3 pairs	73, 133, 198	Bn	m determination
δB_p local Mirnov probe	Midplane	4 pairs	67, 97, 137,167	B_p	Control
Active coil	Midplane	3 pairs	79, 139, 199	Bn	Feedback error field correction

shown later, about one half of the maximum current is used for error field correction. It should be noted that the applied active field does not have any helicity preference, since only one layer of coil exists in the poloidal direction.

The possible performance of these sensors along with control logic has been analyzed with the VALEN code [21] with present coils and possible future upgrade coil locations. Best performance is obtained with the δB_p Mirnov loops located inside the vacuum vessel and the performance with δB_r saddle flux loop located outside the vacuum vessel is predicted to be less effective. The addition of coils located above/below the midplane with δB_p sensor operation should be able to stabilize the RWM up to a value of β_N that is 90% above the $\beta_N^{\text{no wall}}$ and 10% below the $\beta_N^{\text{ideal wall}}$ limit. These results are consistent with other studies by Liu [16] and Chu [17,18].

4. Experimental results of RWM control

The RWM control experiment has been carried out over a wide parameter range, including discharges developed for steady-state advanced tokamak operation [14] where the no-wall limit is $\beta_N \approx 4\ \ell_i$, and discharges where broad current density profiles produced by plasma current ramping reduce the no-wall limit to $\beta_N \approx 2.4\ \ell_i$. Here, we discuss the process of the feedback stabilization studied in the 2.4 ℓ_i regime.

4.1. Comparison of various feedback sensors

Figure 5 shows the observations with internal/external saddle loops with smart shell logic, where the time variation of total flux was minimized by the feedback. The target discharge was produced with a 1.6 MA/s I_p ramp. The fast I_p ramp maintains the low ℓ_i configuration, where modest NBI power is sufficient to reach well above no-wall beta limit. The feedback was applied from 1300 ms. The use of feedback with external sensor loops extended the high beta duration up to 1425 ms. The internal δB_r sensor loop prolonged the duration further to 1480 ms and

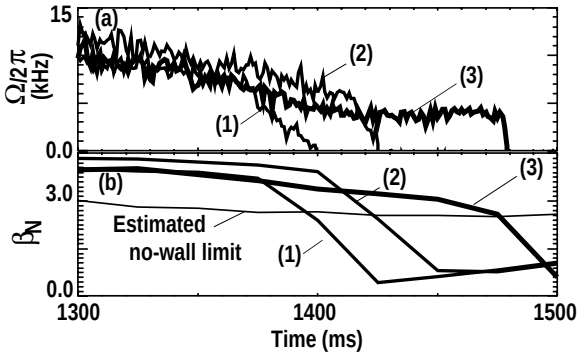

Fig. 5. Comparison of internal and external δB_r sensor operations with smart shell logic. (1) No feedback(105588), (2) External δB_r sensor feedback(105591), (3) Internal δB_r sensor feedback (105596) (a) Rotation frequency at q = 2 surface, (b) I_p vs. time. (b) β_N and the no-wall limit estimated by 2.4 ℓ_i.

the plasma rotation was also maintained. This observation is qualitatively consistent with predictions that the internal loop has advantages, such as, the favorable phase shift of the field reflecting back from the eddy current on the vessel.

The comparison of δB_r and δB_p located inside the vessel is shown in Fig. 6. The advantages of δB_p sensor is the rejection of δB_r component produced by either the active coil or the eddy current excited by the active coil. In this series of experiments, the discharge loses the high beta period at 1380 ms. The δB_p sensor operation extended the discharge to 1580 ms compared to 1440 ms with the δB_r sensor. Since the q-edge was decreasing toward 3, the longer duration means that the discharge faces stronger external kink onset. The requested coil current amplitude and phase of n=1 pattern are shown in Fig. 6(c,d).

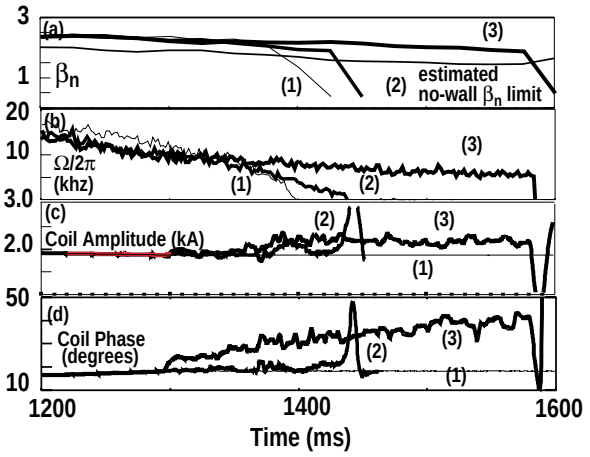

Fig. 6. Comparison of δB_r and δB_p sensors located inside the vessel. (1) Shot (106196) with no feedback, (2) Shot (106187) with the internal δB_r sensor feedback, (3) Shot (106193) with the internal δB_p sensor feedback (a) β_N and ℓ_i (b) Rotation frequency at q = 2 surface (c) Coil current amplitude for the n=1 component (d) Coil current toroidal phase for the n=1 component.

The error field correction was set 2 kA to compensate approximately empirically-determined error field. For the operation of both sensors, the amplitude requested from the feedback stays at approximately 2 kA level, which indicates that the initial estimated coil current was reasonable. However, δB_p sensor shifted the field direction of n=1 about 10–20 degrees immediately after the feedback was turned on. On the other hand, the δB_r sensor did not sense the need for the directional shift. The slight increase of amplitude around 1400 ms could not stabilize the mode, leading to the final collapse. The fine detection of field direction and its adjustment seem to have been the crucial element for stabilizing the RWM.

4.2. High β_N achievement via error field correction by feedback

Once it was determined that the δB_p sensor is superior to other sensors, the long-duration, high β_N, discharge was explored using the internal δB_p sensor. The target discharge was with a modest I_p ramp of 0.6 MA/s. Without feedback the pre-programmed current for error field correction was set to 1 kA with ϕ_c = 7 degrees (Fig. 7). The rotation velocity started to decrease rapidly, similar to the case in Fig 6, due to the increase of the RWM and the β_N decreased gradually

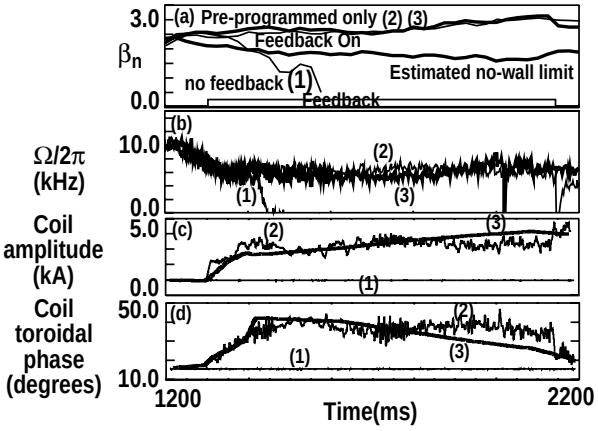

Fig. 7. Comparison with/without optimized error compensation. (1) Shot with no feedback (106530) with pre-programmed non-optimized error correction current (with amplitude of 1 kA and ϕ_c = 7 degrees). (2) Shot with feedback (106532) with pre-programmed non-optimized error correction current (amplitude of 1 kA and ϕ_c = 7 degrees). (3) Shot with feedback shot (106534) with pre-programmed error correction current adapted from the feedback shot (106532) (a) β_N and estimated $\beta_N^{\text{no wall}}$ limit, (b) plasma rotation frequency at q = 3 surface, (c) coil current amplitude for the n=1 component, (d) coil current toroidal phase for the n=1 component.

from 1300 ms (case 1). When the feedback was applied with the same pre-programmed current, the feedback increased immediately the coil current to 2 kA and gradually up to 3–4 kA level and the field direction was shifted to $\phi_c = 40$ degrees. The high beta duration was increased to 2000 ms together with β_N increase to 3.0, which is about twice of $\beta_N^{\text{no wall}}$ and close to $\beta_N^{\text{ideal wall}}$ according to GATO calculation (case 2). When the pre-programmed current was modified to match the coil current obtained by feedback operation (case 2), the time evolution of β_N is identical to the feedback (case 2), and the plasma rotation velocity is also very similar to the results obtained with feedback (case 3).

The comparison of these three types of operations indicates that (1) the feedback process can track the error field with good accuracy, and as a consequence, the n=1 component of error field was determined with the feedback process and (2) the use of the obtained current as error field correction without feedback can produce the high plasma rotation velocity and high β_N configuration. This observation along with discussion in Section 2 on high β_N achievement with higher angular momentum indicates that the higher rotation velocity with better error field correction is the essence of this success.

5. Advancing the RWM control concept

As discussed in the previous section, we have observed that: (1) the stable RWM mode responds to the external field (EFA) toroidally shifted from the applied field angle, (2) the error field can be tracked by a feedback system, and (3) higher beta was achieved up to the ideal MHD limit with higher rotation. These experimental results indicate that magnetic feedback stabilization and stabilization by plasma rotation are not two distinct processes, but that both of them work together in a tightly coupled manner.

Recently, theoretical studies have been carried out on the RWM process including plasma rotation by several groups [22–25]. Here, a simple illustration of the feedback function is shown in Fig. 8(a). Firstly, the EFA (RWM) is excited near the marginal condition. Then the perturbation observed by the sensor requests the active coil current. The feedback responding to the EFA suppresses the mode amplitude and simultaneously reduces the error field, increasing the plasma rotation. Then faster rotation opens a stable path up to the ideal-wall β_N limit. This process is a unified scheme converged from the process proposed by Bondeson [6] and the magnetic feedback process. The difference from traditional RWM feedback is that the coil current energized by the sensor signal simultaneously suppresses the mode and compensates the error field. The path to stable higher beta configuration stays open as long as the rotation velocity is kept above a critical value. It should be also noted that the feedback still is functioning to stabilize the mode even when the sufficient plasma rotation is not available.

The overall feedback process can be described qualitatively with a cylindrical lumped model as was discussed in [26]. The

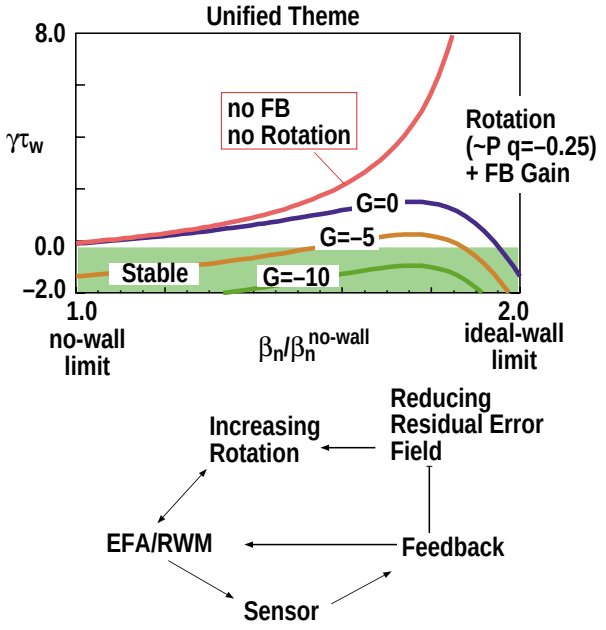

Fig. 8. Schematic of unified theme for RWM control both with feedback and plasma rotation. (a) Schematic diagram and (b) the performance with the unified theme.

main parameter is, L_{eff}, which can represent the pressure balance and the normal magnetic field continuity at the plasma surface.

$$L_{eff}\delta I_p + M_{wp}\delta I_w + M_{cp}\delta I_c = 0 \qquad (1)$$

where, suffixes p, w, c, and o correspond to plasma, passive wall, external (active or error field) coil, and observation sensor respectively. The M_{ij} are mutual inductances between these elements. δI_p, δI_w, and δI_c correspond to the plasma skin current, the passive wall eddy current, and the external coil current respectively. The value, L_{eff}, includes the MHD mode displacement gradient, β_o, defined just inside the plasma surface, and the safety factor through f = m – nq. The formulation can be expanded in order to include the dissipation of the mode due to the plasma rotation and kinetic term for low frequency limit ($\gamma\tau_A < 1$),

$$L_{eff} = (\beta_o - 2/f + 1 + \kappa\Omega_\phi^2 + i\,\alpha\,\Omega_\phi)/ (\beta_o - 2/f - 1 + \kappa\,\Omega_\phi^2 + i\,\alpha\,\Omega_\phi) \qquad (2)$$

This formulation is equivalent to the treatment of the kinetic energy and dissipation term with δw approach in the [24]

$$(\gamma\tau_w + i\Omega\tau_w)^2(\kappa/\tau_w^2) + (\gamma\tau_w + i\Omega\tau_w)(\alpha/\tau_w) + \delta W_p + (\delta W_v^b \gamma\tau_w + \delta W_v^\infty)/ (\gamma\tau_w + 1) = 0 \qquad (3)$$

where the first and second terms represent the impact of plasma rotation and dissipation, and the third term the ideal MHD potential energy. The fourth term is for the effect of finite wall resistivity. The value, Ω_ϕ, is the angular rotational frequency and κ, and α represents the strength of kinetic, and dissipation term relative to the plasma potential energy respectively.

When an external field such as error field exists, the plasma mode response in the quasi steady state is given by

$$\delta I_p = (-M_{cp}/L_{eff})\,\delta I_c \quad . \qquad (4)$$

This simple cylindrical formulation is obtained for a current kink driven RWM with $f_{min} < f \leq 1$ where f=1 and f=f_{min} correspond to current driven kink onset with no-wall and with ideal wall respectively. The model does not include the value β_N. However, we still can discuss the qualitative behavior by relating β_N to f with $\beta_N = 2/f - 1$, when the plasma condition approaches the ideal MHD limit. With this definition, we preserve the fundamental criterion: f=1 as the marginal stability condition for ideal kinks at $\beta_N = \beta_N^{no\,wall}$ and the usual wall-plasma separation determines f_{min} (<1) at $\beta_N = \beta_N^{ideal\,wall}$. A similar relation is also used in [21,27].

Figures 3(c) and (d) show the estimated values for the observed EFA using β_o =1.0, α = 0.002, κ = 5, and experimentally observed plasma rotation. The absolute value of the mode amplitude can not be estimated from the cylindrical mode, mainly due to the limitations imposed by the single pattern assumption in this simple cylindrical model, causing a mismatch of field patterns between the externally-applied and mode fields. The estimated dependence of the toroidal phase shift versus, $\beta_N/\beta_N^{no\,wall}$ seems to be qualitatively consistent with the observations. The large scattering on the estimated values of amplitude and phase can be attributed to too-high of a sensitivity due to the resonant condition and to the uncertainty of the rotational frequency. However, this scattering itself may reflect the hidden parameters of the actual dissipation mechanism, of which details are not included in this simple model.

For completeness in modeling the feedback scheme shown in Fig. 8(a), the time behavior of the plasma rotation must be included. Here, we will use the angular momentum dissipation equation with the electromagnetic torque applied by the external field to the mode on the plasma surface [22,23,25,28] expressed using the lumped parameter approach [26] instead of the commonly used flux discontinuity on the plasma surface.

$$\tau_w^2\,\partial/\partial t(\Omega_\phi) = C_N^{rot}\,\delta I_p\,(M_{pw}\,\delta I_w + M_{pc}\delta I_c)\,[\delta I_p(0)\,\delta I_c(0)]^{-1}\,(M_{pw}\,M_{pc})^{-1/2} \qquad (5)$$

where, $C_N^{rot} = 2\pi\,(a/R)[\,\tau_w^2(\tau_A^{\delta B.p}\,\tau_A^{\delta B.ext})$, and time is normalized to τ_w.

Here, $\tau_A^{\delta B-p}$ and $\tau_A^{\delta B-ext}$ are Alfvén times for magnetic field on the plasma surface produced by $\delta I_p(t=0)$ and $\delta I_c(t=0)$ respectively.

The shell boundary condition provides

$$M_{pw}\partial/\partial t(\delta I_p) + L_w\partial/\partial t(\delta I_w) + M_{wc}\,\partial/\partial t(\delta I_c) + R_c\,\delta I_w = 0 \quad . \quad (6)$$

The active coil current, δI_c, with a current power supply provides

$$\delta I_c = G\,\delta\Psi_0,\ \delta\Psi_0 = M_{op}(\delta I_p) + M_{ow}(\delta I_w) + M_{wc}(\delta I_c) \quad . \quad (7)$$

The Eqs. (2), (5), and (6) correspond to the MHD equations formulated in [23] in the limit of slow time evolution.

The model with Eqs. (2), (6) and (7) was used to calculate the stabilizing effects of rotation and feedback, as shown earlier in Fig. 1. It is important to note that each method has its limitations. Feedback alone [Fig. 1(a)] leads to a stability limit below the ideal-wall limit. Plasmas stabilized by rotation alone may be only weakly stable over a large range of beta values [Fig. 1(b)] and are vulnerable to error fields. However, the model also shows that the combination of rotation and feedback can yield robust stabilization up to the ideal-wall limit [Fig. 8(b)].

Figure 9 shows an example of simulation [with Eqs. (2), (5), (6), and (7)] of the feedback applied after EFA onset with a residual error field. The parameters here are used with the experimental conditions: error field = 0.5 gauss, and τ_w = 5 ms. The initial rotation frequency $\Omega\tau_w = -250$, corresponds to 8 kHz. The dissipation strength parameter, α/τ_w, was adjusted to 0.0015 so that the plasma is marginally unstable up to the ideal wall with the initial velocity. The rotation damping factor C_N^{rot} is set to –5. Without error feedback, the mode grows due to the EFA and the amplitude rapidly increases due to the gradual decrease of plasma rotation. The slow oscillation starts due to the toroidal phase shift

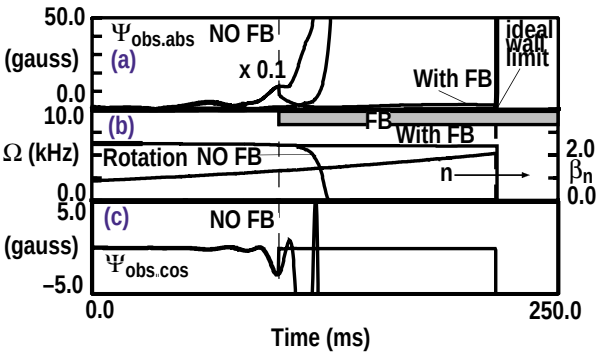

Fig. 9. Feedback simulation with feedback applied at 100 ms. The error field was applied from the t=0 with cos(ϕ) distribution. (a) Absolute value of mode amplitude (with x1 and x 0.1), (b) rotation frequency and β_N,(c) cos(ϕ) component of the mode to show oscillation behavior before the rotational collapse.

around 70–90 ms. When the feedback is applied at t = 100 ms with the poloidal sensor, the mode is suppressed and the termination of high β_N duration occurs due to the ideal-wall limit. The simulation is qualitatively consistent with the experimental observations. The detailed comparative study of these parametric dependencies such as, α/τ_w and C_N^{rot} with experiment will be useful to explore the dissipation mechanism inside the plasma.

6. Summary

We have made substantial progress in the control of one of most dangerous MHD modes for practical rectors, the resistive wall mode. Open loop operation discovered that at $\beta_N \approx \beta_N^{no\ wall}$, the marginally stable RWM responds in a resonant manner to the applied field with the toroidal phase shift relative to the applied field as predicted by Boozer. This toroidal phase shift is a surprising contrast to the rigid shift for the n=0 vertical position control for non-circular plasmas. The accurate tracking of the residual error field took place through the feedback process. When sufficient angular momentum injection is available, $\beta_N \approx \beta_N^{ideal\ wall}$, can be achieved by sustaining the plasma rotation.

From the hardware point of view, this accurate error field tracking was made possible by the use of the internal δB_p sensor. The internal δB_p sensor was able to detect the mode to within 20 degrees accuracy, which

external sensors have failed so far to achieve. Accurate error field compensation has been the key of success of opening a path of the exploration up to the ideal MHD limit.

A simple simulation can provide qualitative behavior of EFA and the feedback operation. This indicates that, although the RWM feedback process is complex, a few fundamental parameters may play significant roles on the process.

These series of successes encourage new challenges. For example, It will be extremely useful to assess whether any improvement of external sensors and logic can perform to the same level of accuracy for mode tracking, since the external sensor is advantageous for reactor applications. Secondly, this new unified scheme to higher β_N will require more knowledge of the dissipation mechanism and the rotation damping process due to the RWM mode amplitude and residual error field. The physics of angular momentum loss mechanism should be explored over a wide range of physical parameters. Thirdly, the RWM stabilization of plasmas with no rotation or well below the critical rotation should be explored to make much wider the parameter regime available to higher β_N operation.

Finally, on DIII-D device, based on these observations along with the prediction by VALEN code, twelve additional off-mid plane coils will be installed. Various operating plasma regimes will be challenged up to $\beta_N^{\text{ideal wall}}$ limit in very near future.

7. Acknowledgments

This work is supported by the U.S. Department of Energy Grant DE-FG02-89ER53297 and Contracts DE-AC03-99ER54463, DE-AC05-00OR22725, and DE-AC02-76H03073. We are greatly thankful to physicists, engineering staffs, technical staffs involved in this project. In particular, we would like to express our appreciation to DIII-D operation group.

References

[1] T.S. Taylor, et al., Phys. Plasmas **2**, 2390 (1995).
[2] M. Okabayashi, et al., Nucl. Fusion **36** 1167 (1996).
[3] T. Ivers, et al., Phys. Plasmas **3**, 1926 (1996).
[4] J. Freidberg, *Ideal Magneto-Hydrodymanics* (Plenum, New York, 1987), Chapter 9.
[5] R. Fitzpatrick and T. Jensen, Phys. Plasmas **2**, 2641 (1996).
[6] A. Bondeson and D. Ward, Phys. Rev. Lett. **72**, (1994) 2709.
[7] D. J. Ward and A. Bondeson, Phys. Plasmas **2**,1570(1995)
[8] M. Okabayashi et al., Phys. Plasmas **8**, 2071 (2001).
[9] A.M. Garofalo et al., Phy. Plasmas (APS invited paper, accepted); A.M. Garofalo, R.J. La Haye, and J.T. Scoville, "I need a title here," to be submitted to Nucl. Fusion.
[10] A.M. Garofalo et al., Nucl. Fusion **41**, 1171 (2001).
[11] A. Boozer, Phy. Rev. Lett. **86**, 1176 (2001).
[12] A.M. Garofalo et al., Phys. Rev. Lett. **82**, 3811 (1999).
[13] L. Johnson et al., in "Structure and Feedback Stabilization of Resistive Wall Modes in DIII-D," in Proc. of the 28th EPS Conf. on Controlled Fusion and Plasma Physics, Madeira, 2001 (European Physical Society, Petit-Lancy, 2001) to be published.
[14] M.R. Wade " Physics of High Bootstrap Fraction, High Performance Plasmas on the DIII-D Tokamak," in Proc. of the 28th EPS Conf. on Controlled Fusion and Plasma Physics, Madeira, 2001 (European Physical Society, Petit-Lancy, 2001) to be published.
[15] Y.O. Liu and A. Bondeson, Phys. Rev. Lett. **84**, 907 (2000).
[16] Y.Q. Liu, et al., Phys. Plasmas **7**, 3681 (2000).

[17] M.S. Chu et al., "Modeling of Feedback Stabilization of the Resistive Wall Mode in General Geometry," in Proc. of the 28th EPS Conf. on Controlled Fusion and Plasma Physics, Madeira, 2001 (European Physical Society, Petit-Lancy, 2001) to be published.
[18] M.S. Chance et al., "Theoretical Modeling of the Feedback Stabilization of External MHD Modes in Toroidal Geometry," Nucl. Fusion (accepted).
[19] E.J. Strait et al., Phys. Rev. Lett. **74**, 2483 (1994).
[20] A.M. Garofalo, et al., Nucl. Fusion **40**, 1491 (2000).
[21] J. Bialek et al., Phys. Plasmas **8**, 2170 (2001).
[22] R. Fitzpatrick and A. Aydmir, Nucl. Fusion **36**, 11 (1996).
[23] R. Fizpatrick, "A Simple Model of the Resistive Wall Mode in Tokamaks," (private communication).
[24] M.S. Chu et al., Phys. Plasmas **2**, 2236 (1995).
[25] A. Boozer, Phys. Plasmas **6**, 3180 (1999).
[26] M. Okabayashi, N. Pomphrey and R. Hatcher, Nucl. Fusion **38**, 1607 (1998).
[27] A. Boozer, Phys. Plasmas **9**, 3350 (1998).
[28] S.C. Guo and M.S. Chu, Phys. Plasmas **8**, 3342 (2001).